

Heteroarylisopropylamines as MAO inhibitors

Gabriel Vallejos,^a Angélica Fierro,^a Marcos Caroli Rezende,^{a,*}
Silvia Sepúlveda-Boza^b and Miguel Reyes-Parada^b

^a*Facultad de Química y Biología, Universidad de Santiago, Casilla 40, Correo 33, Santiago, Chile*

^b*Facultad de Ciencias Médicas, Universidad de Santiago, Casilla 442, Correo 2, Santiago, Chile*

Received 6 January 2005; revised 18 April 2005; accepted 18 April 2005

Available online 23 May 2005

Abstract—The in vitro monoamine oxidase inhibitory (MAOI) activities of 11 heteroarylisopropylamines vis-à-vis MAO-A and MAO-B were described and interpreted in terms of possible interactions with the enzyme active site. Molecular dynamics simulations allowed a comparison between the most active MAO-A inhibitor of the series, the 1-(2-benzofuryl)-2-aminopropane, and the specific, analogous MAO-A substrate serotonin.

© 2005 Elsevier Ltd. All rights reserved.

1. Introduction

Considerable progress has been made in the past years in deciphering the mechanisms of action and inhibition of MAO. The human MAO-B isoform has been crystallized with a variety of inhibitors.^{1–3} The structure of a rat MAO-A bound with clorgyline has been recently elucidated from X-ray diffraction analysis.⁴ These developments have made possible a more detailed understanding of the binding between monoamine oxidase inhibitors and the protein. Computational simulations coupled with structure–activity studies may now be used to mimic interactions in the active site of the enzyme and to understand the subtle factors, that govern MAO inhibitory activity and selectivity.⁵

SAR studies on the activity and selectivity of arylalkylamines as MAO inhibitors have been a subject of recent interest.^{6–9} Our previous QSAR studies of substituted phenylisopropylamines have identified some features responsible for an increased monoamine oxidase inhibitory (MAOI) activity.^{6,7} Soft, lipophilic thioalkyl substituents at position 4 of the aromatic ring tended to increase their activity. The fact that the

introduction of electron-withdrawing substituents like nitro, trifluoromethyl, alkylsulfoxyl and sulfonyl, markedly reduced their MAOI activity was taken as an indication of possible HOMO–LUMO interactions between these compounds and aromatic fragments at the active site.⁶

Replacement of an aryl by a heteroaryl group has led in some cases to interesting, novel MAO inhibitors. This, for instance, was the case of a 5-hydroxyindole derivative related to pargyline, which was found to be more potent and selective than the MAO-A inhibitor clorgyline.¹⁰ For a series of aryloxazolidinones, the introduction of a benzothiazolyl ring led to a potent and selective MAO-A inhibitor.^{11,12}

As a natural extension of our studies on arylalkylamines, we decided to evaluate some heteroaromatic systems and compare their activity with that of their homoaromatic analogues. A few thienyl derivatives had been assessed in vitro previously as MAO inhibitors.¹³ Some chlorinated derivatives showed a moderate to good (20–70%) MAO inhibition at 0.2 μ M concentration. Since then, no other studies have appeared in the literature dealing with the MAOI activity of this family of compounds.

Our previous work with substituted arylalkylamines emphasized the importance of interactions between the aromatic rings of the pharmacophore and the hydrophobic fragments in the active site of the enzyme.^{6,7}

Keywords: MAO inhibitors; Heteroarylisopropylamines; Molecular dynamics simulation.

* Corresponding author. Tel.: +56 2 681 2575; fax: +56 2 681 2108; e-mail: mcaroli@lauca.usach.cl

The present report, dealing with heteroaromatic systems, aims at contributing to a better understanding of these interactions by taking advantage of the recently elucidated structure of the MAO isoforms.

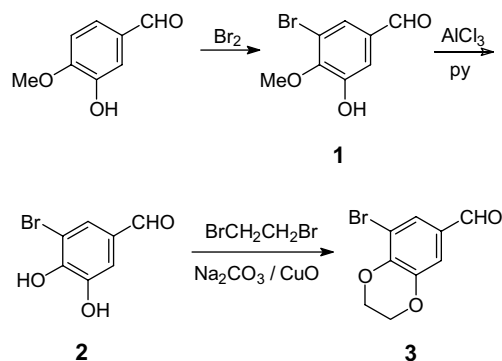
2. Results

The racemic heteroarylaminopropanes, obtained in the form of the hydrochloride salts **15–25**, were prepared from the corresponding heteroarylcarboxaldehydes by conversion into the intermediate nitropropenes **4–14** and reduction with lithium aluminium hydride.

$\text{Het-CHO} \xrightarrow[\text{BuNH}_2]{\text{EtNO}_2} \text{Het-CH=CH-NO}_2 \xrightarrow[\text{ii) HCl}]{\text{i) LiAlH}_4} \text{Het-CH}_2\text{-CH}_2\text{-NH}_2\cdot\text{HCl}$		
Het	4–14	15–25
	4	15
	5	16
	6	17
	7	18
	8	19
	9	20
	10	21
	11	22
	12	23
	13	24
	14	25

Most aldehydes were commercial. An exception was 3-bromo-4,5-ethylenedioxybenzaldehyde, which was prepared from 4-hydroxy-3-methoxybenzaldehyde (vanillin) by the route below.

The prepared heteroarylaminopropanes were assayed *in vitro* as inhibitors of the two MAO isoforms. The



obtained MAOI activities, expressed as IC_{50} values, are given in Table 1. For the sake of comparison, the percentage of MAO inhibition at 100 μM (the highest concentration of the inhibitors tested) is also given for all compounds with an $\text{IC}_{50} > 100$.

The possible time-dependence of MAO inhibitory activity was assessed by preincubating the reaction mixture with different compounds at appropriate concentrations for 30 min, and then measuring the enzymatic activity. Table 2 shows the results obtained for some representative compounds after preincubation (0 and 30 min) with MAO-A.

3. Discussion

Inspection of Table 1 shows that most of the heteroarylaminopropanes are selective MAO-A inhibitors. Among the best inhibitors (IC_{50} values < 100), the only exception was compound **22**, which exhibited, in addition to its MAO-A inhibitory activity, an interesting MAO-B inhibitory activity. Such selectivity is shared with the majority of other previously evaluated 1-aryl-2-amino- propanes.^{6,7,14,15}

Thienyl derivatives were in general better MAO-A inhibitors than their furyl analogues. This emerges from a comparison of pairs **17/19** and **22/23** in Table 1. Also, among the less active compounds ($\text{IC}_{50} > 100$), the 3-thienyl derivative **18** is a better inhibitor (30% inhibition) than the furyl analogue **20** (18% inhibition) at a 100 μM concentration. This trend parallels the greater MAO-A inhibitory activity in the series of 1-aryl-2-aminopropanes of compounds substituted with a thioalkyl group, when compared with their oxygen analogues.^{6,14} Substitution by sulfur renders an aromatic ring softer and more polarizable than analogous substitution by oxygen. Hydrogen-bond formation with the hard oxygen atom is also greatly diminished in a sulfur analogue.

Substitution of the heteroaromatic (thienyl or furyl) ring with a bromine atom led to an improvement of the inhibitory activity of the parent aminopropanes, as can be seen in a comparison of compounds **21** and **22** with **17** or **23** with **19** in Table 1. A similar trend had been reported for ring-chlorinated thienylisopropylamine deriva-

Table 1. In vitro MAO-A and MAO-B inhibitory activities of aminopropane hydrochlorides **15–25**

Compd	Heteroaryl group	IC ₅₀ (μM) ^a	
		MAO-A	MAO-B
15	3,4-Ethylenedioxyphenyl	11.0 ± 2.4	>100 [16.4] ^b
16	3,4-Ethylenedioxy-5-bromophenyl	18.3 ± 3.0	>100 [26.2] ^b
17	2-Thienyl	64.4 ± 4.0	>100 [31.5] ^b
18	3-Thienyl	>100 [30.1] ^b	>100 [32.4] ^b
19	2-Furyl	>100 [20.6] ^b	Inactive [0] ^b
20	3-Furyl	>100 [18.3] ^b	>100 [18.0] ^b
21	4-Bromo-2-thienyl	17.8 ± 0.4	>100 [36.0] ^b
22	5-Bromo-2-thienyl	15.8 ± 1.6	12.9 ± 0.5
23	5-Bromo-2-furyl	44.8 ± 0.8	>100 [12.5] ^b
24	3-Benzothienyl	16.2 ± 0.4	>100 [36.5] ^b
25	2-Benzofuryl	0.8 ± 0.1	>100 [34.0] ^b

^a Compounds described as inactive were completely devoid of activity at a 100 μM concentration; compounds showing less than 50% inhibition at this concentration are reported with IC₅₀ >100.

^b Values between square brackets correspond to the percentage of MAO inhibition at a 100 μM concentration of the inhibitor.

Table 2. MAO-A inhibition after preincubation with compounds **22**, **23** and **25**

Compd [concn, M]	% Inhibition of MAO-A ^a	
22 [10 ^{−5}]	49.3 ± 4.9 ^b	56.0 ± 2.8 ^c
23 [5 × 10 ^{−5}]	58.5 ± 7.2 ^b	61.1 ± 0.2 ^c
25 [10 ^{−6}]	60.5 ± 0.7 ^b	59.5 ± 3.5 ^c

^a Average values of three measurements.

^b After 0 min of preincubation.

^c After 30 min of preincubation.

tives.¹³ This effect might be explained on the basis of an increased polarizability induced by the introduction of a halogen atom on the ring. An increased polarizability could also explain the greater MAO-A inhibitory activity of the benzo derivatives **24** and **25**, when compared with **18** and **19**, respectively.

Negligible changes in MAO-A inhibition were observed after different preincubation times (0 and 30 min, Table 2), indicating that blockade of the enzyme was not time-dependent, and that the inhibition was not due to substrate competition. These experiments showed that compounds **22**, **23** and **25** were not metabolized by the enzyme and that the observed inhibition resulted from a real blockade of the enzymatic activity. The present results agree with similar observations reported previously by us for several other arylisopropylamine derivatives.^{14,15}

The structural requirements leading to an enhanced MAOI activity in the series of prepared heteroarylaminopropanes parallel similar observations with other arylaminopropanes. We had previously investigated the hypothesis of charge-transfer interactions between the aromatic ring of these inhibitors and the flavin cofactor in determining the MAOI activity of these compounds.⁶ The crystallographic elucidation of the interactions between some inhibitors and the FAD cofactor in the active site of MAO-B^{1–3} and MAO-A⁴ made this hypothesis no longer tenable.⁵ However, the obtained correlations of MAO-A inhibitory activity with the frontier orbital energies of the inhibitors⁶ may reflect

charge-transfer interactions with other aromatic fragments in the active site. This possibility gains support from the present study, where a soft, polarizable heteroaromatic ring showing an extended conjugation, like compound **25**, was found to be the best MAO-A inhibitor of the series. In order to gain some insight into these hypothetical interactions, we carried out simulations with this compound in the active site of the enzyme.

Due to the presence of a chiral centre on the arylaminopropane structures, both enantiomers of the benzofurylalkylamine **25** were docked into the active site of MAO-A by using the crystallographic data available for the rat enzyme isoform (1O5W).¹⁶

The benzofuran ring in both isomers inserted itself into a hydrophobic pocket formed by residues, which included Tyr407, Tyr444, Gln215 and Phe208. The molecules were further stabilized by hydrogen bonds between the side-chain amino group and neighbouring amino acids, like Thr336 for the *S*-enantiomer and Phe208 and Asn181 for the *R*-isomer.

The heterocyclic ring system in **25** is related with the indolyl group present in 5-HT, a specific substrate of MAO-A. This structural similarity might suggest similar interactions between the two heterocyclic systems and the hydrophobic cavity of MAO-A. In Figure 1 we superimpose the structures of the *S*-benzofuryl derivative **25** and 5-HT, after docking both compounds into the enzyme active site.

As can be seen, both heterocyclic rings occupy the same region of the cavity, with one important difference. While the side-chain amino group of serotonin approaches the FAD ring system, hydrogen bonding with ring N5, the corresponding amino group of **25** points away from the flavin ring, forming a hydrogen bond with Thr336. A similar difference in side-chain orientation occurs for 5-HT and the *R*-isomer of **25** (not shown). Thus, different alignments are obtained for the two heterocyclic compounds, with their ring systems sharing the same region and similar interactions with the aromatic fragments of the hydrophobic cavity.

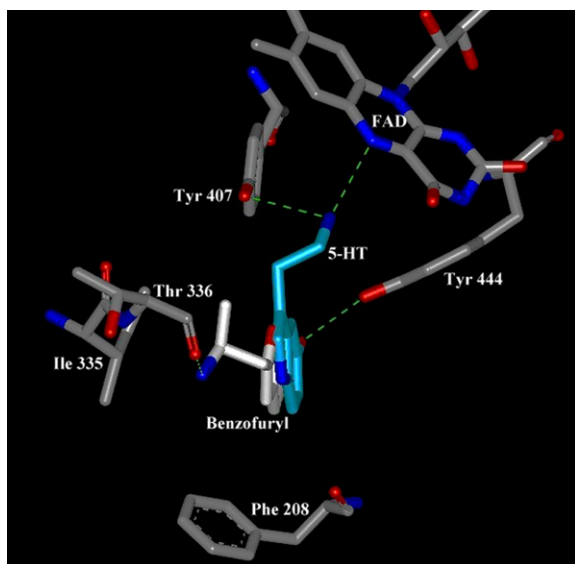


Figure 1. Superimposed structures of 5-HT (blue) and the *S*-enantiomer of **25** (white), docked into the active site of rat MAO-A (grey fragments), showing the different orientations of the side chains of both compounds. The 5-hydroxy group of the 5-HT indole ring hydrogen bonds with the phenolic OH substituent of Tyr 444, and its side-chain amino group forms bonds with the flavin N5 and Tyr407. By contrast, the side-chain amino group of compound **25** interacts with Thr336.

Therefore, in spite of occupying the active site and consequently blocking access of any substrate to the flavin ring, the benzofuryl derivative **25** would avoid deamination by preferring a different side-chain orientation with respect to the FAD cofactor. This result provides a rationale for the observed inhibitory activity. This proposal is supported by the lack of substrate behaviour shown by **22**, **23** and **25** (Table 2) as evaluated in preincubation studies.

An 85–88% identity is observed between the same isoforms (MAO-A or MAO-B) from human and rat,¹⁷ and a high homology at the active site of MAO-B from both species could be inferred from the analysis of their primary sequences. This allows, in principle, an analysis of the structural mechanisms underlying the selectivity shown by our compounds (data obtained with the rat isoform), using the available crystallographic data (rat MAO-A and human MAO-B). With this aim, the active site of MAO-B was superimposed onto the corresponding site of MAO-A already docked with **25** (Fig. 2). As can be seen, the presence of Tyr326 in MAO-B (Ile335 being the corresponding residue in MAO-A), would prevent the accommodation of **25** into the active site of MAO-B. This suggests a possible explanation for the selectivity exhibited by this compound. It is worth pointing out that fragments Ile335 and Tyr326 in MAO-A and MAO-B, respectively, have been regarded as major determinants of selectivity for both substrates and inhibitors.^{4,18,19}

The results from our simulations should be regarded with caution, firstly because biochemical data obtained using rat enzymes were analysed with the assumption

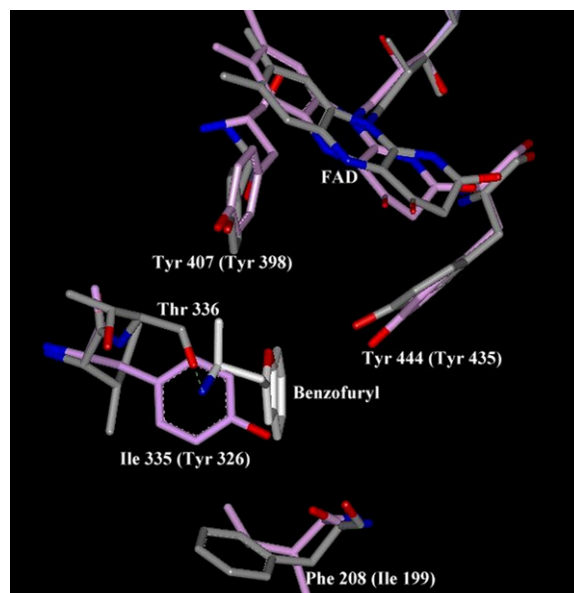


Figure 2. Superimposed binding sites of rat MAO-A (grey) and human MAO-B (pink fragments). The *S*-enantiomer of **25** is shown in white. Steric repulsion with Tyr326 in MAO-B would prevent accommodation of the inhibitor in the enzyme active site. Such interactions are not present with the corresponding MAO-A fragment Ile335.

of a high similarity between the active sites of rat and human MAO-B. Mutation of specific residues in MAO from both species has not always resulted in identical functional changes.^{19,20} Likewise, the conclusions from docking studies regarding the inhibitory mechanism are limited because they were obtained using the enantiomers of **25** and not its racemate. Further experiments assessing the inhibitory properties of both optical isomers of aminopropane derivatives are necessary to confirm the computational predictions. Despite these limitations, our results and conclusions highlight the usefulness of coupling computational simulations with structure–activity studies in order to understand the subtle factors governing MAO inhibitory activity.

4. Experimental

¹H and ¹³C NMR spectra were recorded on a Bruker Avance 400 MHz instrument, employing tetramethylsilane as internal standard. IR spectra were obtained with a Perkin Elmer 750 spectrometer. Melting points were measured with a Microthermal apparatus and were not corrected.

The following aldehydes were purchased from Aldrich: 4-hydroxy-3-methoxybenzaldehyde, 3,4-ethylenedioxybenzaldehyde, 2- and 3-thiophenecarboxaldehydes, 2- and 3-furancarboxaldehydes, 4- and 5-bromo-2-thiophenecarboxaldehydes, 5-bromo-2-furancarboxaldehyde, 3-benzothiophenecarboxaldehyde and 2-benzofurancarboxaldehyde. 3-Bromo-4-hydroxy-5-methoxybenzaldehyde (**1**) was prepared in 54% yield by bromination of 4-hydroxy-3-methoxybenzaldehyde (vanillin) in acetic acid,²¹ mp 162–163 °C, lit.²¹ mp 158 °C.

4.1. 3-Bromo-4,5-dihydroxybenzaldehyde (2)

To a stirred solution of 3-bromo-4-hydroxy-5-methoxybenzaldehyde (15 g, 65 mmol) in chloroform (150 mL), cooled in a water bath (5–10 °C), was added AlCl_3 (12.4 g, 93 mmol) followed by careful, dropwise addition of pyridine (23 mL). The resulting green solution was refluxed with stirring for 24 h. The deep violet solution was then concentrated by distillation of the solvent. To the cooled dark residue was then added HCl 3 M until the reaction mixture was acidic, and the solid that separated was triturated, washed with acid and filtered to give, after recrystallization in aqueous ethanol, 11.7 g (83% yield) of the 3-bromo-4,5-dihydroxybenzaldehyde, mp 230–232 °C, lit.²² mp 230 °C. IR (KBr) ν_{max} 3250, 3020, 1650, 1590, 1310 and 1000 cm^{-1} . ^1H NMR (CDCl_3) δ 10.30 (2H, br s, OH), 9.70 (1H, s, CHO); 7.10 (1H, d, $J = 2.0$ Hz, H-2); 6.92 (1H, d, $J = 2.0$ Hz, H-5).

4.2. 3-Bromo-4,5-ethylenedioxybenzaldehyde (3)

The preparation employed CuO as catalyst, which was prepared as follows: To a solution of $\text{CuSO}_4 \cdot 5\text{H}_2\text{O}$ (3.13 g, 12.5 mmol) in water (50 mL), heated at 80–90 °C, was added with stirring a solution of NaOH (1.1 g, 27.5 mmol) in water (25 mL). The precipitate was filtered and washed thoroughly with water, and then dried in an oven at 200 °C for 3 h.

A mixture of 3-bromo-4,5-dihydroxybenzaldehyde (1.1 g, 4.8 mmol), 1,2-dibromoethane (0.64 mL, 7.4 mmol), anhydrous Na_2CO_3 (2.3 g, 21.8 mmol) and CuO (0.15 g, 1.8 mmol) in DMF (6 mL) was heated at 120–130 °C for 4 h. The cooled mixture was then acidified with dilute HCl (5%, 20 mL) and extracted with dichloromethane (3 \times 20 mL). The organic extracts were rotary evaporated and the residue purified by column chromatography, employing CH_2Cl_2 as eluent. The 3-bromo-4,5-ethylenedioxybenzaldehyde was obtained as a white solid, 35% yield, mp 77–79 °C. ^1H NMR (CDCl_3) δ 9.71 (1H, s, CHO); 7.60 (1H, d, $J = 2.3$ Hz, H-2); 7.30 (1H, d, $J = 2.3$ Hz, H-6); 4.38 (2H, m, $\text{OCH}_2\text{CH}_2\text{O}$); 4.25 (2H, m, $\text{OCH}_2\text{CH}_2\text{O}$). ^{13}C NMR (CDCl_3) δ 189.64, 146.29, 144.60, 130.46, 127.45, 117.65, 111.63, 65.46 and 63.94.

4.3. Preparation of 1-heteroaryl-2-nitropropenes 4–14. General procedure

A solution of nitroethane (1.6 mL, 22.4 mmol), *n*-butylamine (0.9 mL, 9.1 mmol) and the corresponding heteroarylcarboxaldehyde (7.9 mmol) in acetic acid (4 mL) was heated at 80 °C for 2 h. The crude product that separated on cooling was filtered and recrystallized from methanol, and had its structure confirmed by its ^1H and ^{13}C NMR spectra.

In this way the following nitropropenes were prepared.

4.3.1. 1-(3,4-Ethylenedioxyphenyl)-2-nitropropene (4). Yield 65%, yellow crystals, mp 97–98 °C. IR (KBr) ν_{max} 1620, 1580, 1520, 1300, 1260 and 900 cm^{-1} ; ^1H NMR

(CDCl_3) δ 8.00 (1H, s, $\text{CH}=\text{C}(\text{Me})\text{NO}_2$); 6.90 (3H, m, Ar-H); 4.30 (4H, s, $\text{OCH}_2\text{CH}_2\text{O}$); 2.35 (3H, s, $\text{CH}=\text{C}(\text{CH}_3)\text{NO}_2$). ^{13}C NMR (CDCl_3) δ 146.09, 145.39, 143.62, 133.40, 125.54, 124.27, 119.01, 117.78, 64.53, 64.16 and 14.05.

4.3.2. 1-(3,4-Ethylenedioxy-5-bromophenyl)-2-nitropropene (5). Yield 82%, yellow crystals, mp 140–142 °C. IR (KBr) ν_{max} 2950, 1680, 1600, 1580, 1500, 1300, 1160 and 850 cm^{-1} . ^1H NMR (CDCl_3) δ 7.94 (1H, s, $\text{CH}=\text{C}(\text{Me})\text{NO}_2$); 7.29 (1H, d, $J = 1.7$ Hz, H-6); 7.05 (1H, d, $J = 1.7$ Hz, H-2); 4.45 (2H, m, $\text{OCH}_2\text{CH}_2\text{O}$); 4.35 (2H, m, $\text{OCH}_2\text{CH}_2\text{O}$); 2.45 (3H, s, $\text{CH}=\text{C}(\text{CH}_3)\text{NO}_2$). ^{13}C NMR (CDCl_3) δ 146.80, 144.24, 142.32, 131.91, 126.86, 125.71, 118.26, 110.70, 65.07, 63.92 and 13.86.

4.3.3. 1-(2-Thienyl)-2-nitropropene (6). Yield 79%, yellow crystals, mp 65–67 °C, lit.¹³ 69 °C. ^1H NMR (CDCl_3) δ 8.23 (1H, s, $\text{CH}=\text{C}(\text{Me})\text{NO}_2$); 7.58 (1H, d, $J = 5.1$ Hz, H-5); 7.36 (1H, d, $J = 3.6$ Hz, H-3); 7.12 (1H, dd, $J = 5.1$ Hz, $J' = 3.6$ Hz, H-4); 2.48 (3H, s, $\text{CH}=\text{C}(\text{CH}_3)\text{NO}_2$).

4.3.4. 1-(3-Thienyl)-2-nitropropene (7). Yield 89%, yellow crystals, mp 73–75 °C. IR (KBr) ν_{max} 3100, 1650, 1560, 1500, 1300, 1280 and 800 cm^{-1} . ^1H NMR (CDCl_3) δ 8.08 (1H, s, $\text{CH}=\text{C}(\text{Me})\text{NO}_2$); 7.60 (1H, dd, $J = 2.9$ Hz, $J' = 1.3$ Hz, H-2); 7.44 (1H, dd, $J = 5.0$ Hz, $J' = 2.9$ Hz, H-5); 7.28 (1H, dd, $J = 5.0$ Hz, $J' = 1.3$ Hz, H-4); 2.49 (3H, s, $\text{CH}=\text{C}(\text{CH}_3)\text{NO}_2$).

4.3.5. 1-(2-Furyl)-2-nitropropene (8). Yield 81%, yellow crystals, mp 46–47 °C. IR (KBr) ν_{max} 3100, 1640, 1480, 1500, 1280 and 750 cm^{-1} . ^1H NMR (CDCl_3) δ 7.87 (1H, s, $\text{CH}=\text{C}(\text{Me})\text{NO}_2$); 7.66 (1H, d, $J = 1.7$ Hz, H-5); 6.84 (1H, d, $J = 3.5$ Hz, H-3); 6.60 (1H, dd, $J = 3.5$ Hz, $J' = 1.7$ Hz, H-4); 2.60 (3H, s, $\text{CH}=\text{C}(\text{CH}_3)\text{NO}_2$).

4.3.6. 1-(3-Furyl)-2-nitropropene (9). Yield 73%, yellow crystals, mp 84–85 °C. IR (KBr) ν_{max} 3100, 1640, 1500, 1160 and 800 cm^{-1} . ^1H NMR (CDCl_3) δ 7.93 (1H, s, $\text{CH}=\text{C}(\text{Me})\text{NO}_2$); 7.76 (1H, br s, H-5); 7.53 (1H, br s, H-2); 6.64 (1H, br s, H-4); 2.44 (3H, s, $\text{CH}=\text{C}(\text{CH}_3)\text{NO}_2$). ^{13}C NMR (CDCl_3) δ 146.21, 145.18, 124.63, 119.23, 110.46, 110.05 and 14.19.

4.3.7. 1-(4-Bromo-2-thienyl)-2-nitropropene (10). Yield 86%, yellow crystals, mp 87–88 °C. IR (KBr) ν_{max} 3100, 1640, 1500, 1300, 1160 and 800 cm^{-1} . ^1H NMR (CDCl_3) δ 8.14 (1H, s, $\text{CH}=\text{C}(\text{Me})\text{NO}_2$); 7.51 (1H, s, H-5); 7.31 (1H, s, H-3); 2.55 (3H, s, $\text{CH}=\text{C}(\text{CH}_3)\text{NO}_2$). ^{13}C NMR (CDCl_3) δ **145.98, 136.34, 135.93, 128.52, 125.69, 111.99 and 14.45.**

4.3.8. 1-(5-Bromo-2-thienyl)-2-nitropropene (11). Yield 78%, yellow crystals, mp 138–140 °C. IR (KBr) ν_{max} 3100, 1620, 1480, 1300, 1400, 1280 and 800 cm^{-1} . ^1H NMR (CDCl_3) δ 8.16 (1H, s, $\text{CH}=\text{C}(\text{Me})\text{NO}_2$); 7.17 (2H, s, H-3 and H-4); 2.49 (3H, s, $\text{CH}=\text{C}(\text{CH}_3)\text{NO}_2$). ^{13}C NMR (CDCl_3) δ 144.80, 136.90, 135.14, 131.27, 126.76, 119.92 and 14.47.

4.3.9. 1-(5-Bromo-2-furyl)-2-nitropropene (12). Yield 82%, yellow crystals, mp 91–93 °C. IR (KBr) ν_{\max} 2959, 1729, 1651, 1496, 1301, 1022, 940 and 797 cm^{-1} . ^1H NMR (CDCl_3) δ 8.16 (1H, s, $\text{CH}=\text{C}(\text{Me})\text{NO}_2$); 6.76 (1H, d, $J = 3.5$ Hz, H-4); 6.52 (1H, d, $J = 3.5$ Hz, H-3); 2.56 (3H, s, $\text{CH}=\text{C}(\text{CH}_3)\text{NO}_2$). ^{13}C NMR (CDCl_3) δ 149.93, 131.06, 127.48, 121.20, 119.62, 115.23 and 14.26.

4.3.10. 1-(3-Benzothienyl)-2-nitropropene (13). Yield 84%, yellow crystals, mp 110–112 °C. IR (KBr) ν_{\max} 1620, 1580, 1500, 1300, 1200 and 800 cm^{-1} . ^1H NMR (CDCl_3) δ 8.33 (1H, s, $\text{CH}=\text{C}(\text{Me})\text{NO}_2$); 7.89 (2H, m, H-4 and H-7); 7.67 (1H, s, H-2); 7.47 (2H, m, H-5 and H-6); 2.53 (3H, s, $\text{CH}=\text{C}(\text{CH}_3)\text{NO}_2$).

4.3.11. 1-(2-Benzofuryl)-2-nitropropene (14). Yield 75%, yellow crystals, mp 104–105 °C. IR (KBr) ν_{\max} 3072, 1656, 1516, 1312, 1139, 985 and 748 cm^{-1} . ^1H NMR (CDCl_3) δ 7.94 (1H, s, $\text{CH}=\text{C}(\text{Me})\text{NO}_2$); 7.64 (1H, d, $J = 7.7$ Hz, H-4); 7.53 (1H, d, $J = 8.4$ Hz, H-7); 7.42 (1H, dd, $J = 8.4$ Hz, $J' = 7.4$ Hz, H-6); 7.30 (1H, dd, $J = 7.7$ Hz, $J' = 7.4$ Hz, H-5); 7.13 (1H, s, H-3); 2.73 (3H, s, $\text{CH}=\text{C}(\text{CH}_3)\text{NO}_2$). ^{13}C NMR (CDCl_3) δ 156.32, 149.65, 147.09, 127.94, 127.40, 124.02, 122.19, 121.03, 115.45, 111.82 and 14.63.

4.4. 1-(3,4-Ethylenedioxyphenyl)-2-aminopropane hydrochloride (15)

To a stirred suspension of lithium aluminium hydride (1.20 g, 31.6 mmol) in dry THF (10 mL) was added a solution of 1-(3,4-ethylenedioxyphenyl)-2-nitropropene (**4**) (0.72 g, 3.26 mmol) in dry THF (15 mL). The resulting mixture was refluxed for 3 h. The excess hydride was then decomposed by careful addition of water, the mixture was extracted with diethyl ether (3 \times 15 mL), the organic extracts were dried over MgSO_4 and rotary evaporated. The residue was then dissolved in dry diethyl ether and the hydrochloride (**15**) precipitated by passing gaseous HCl through the solution. Yield 50%, mp 167–170 °C. HRMS m/z 193.0822, calcd for $\text{C}_{11}\text{H}_{15}\text{NO}_2$ 193.1103. Anal. Calcd for $\text{C}_{11}\text{H}_{15}\text{NO}_2\cdot\text{HCl}\cdot 1/2\text{H}_2\text{O}$: C, 55.34; H, 6.77; N, 5.87. Found: C, 55.39; H, 6.50; N 6.31. IR (KBr): ν_{\max} 2900, 1600, 1520, 1300, 1200 and 1080 cm^{-1} . ^1H NMR ($\text{DMSO}-d_6$) δ 8.22 (3H, s, NH_3^+); 6.77 (1H, d, $J = 8.1$ Hz, H-5); 6.73 (1H, d, $J = 2.1$ Hz, H-2); 6.65 (1H, dd, $J = 8.1$ Hz, $J' = 2.1$ Hz, H-6); 4.19 (4H, s, CH_2O); 3.29 (1H, m, $\text{CH}_2\text{CH}(\text{CH}_3)\text{NH}_3^+$); 2.92 (1H, m, $\text{CH}_2\text{CH}(\text{CH}_3)\text{NH}_3^+$); 2.52 (1H, m, $\text{CH}_2\text{CH}(\text{CH}_3)\text{NH}_3^+$); 1.10 (3H, d, $J = 6.5$ Hz, $\text{CH}_2\text{CH}(\text{CH}_3)\text{NH}_3^+$). ^{13}C NMR ($\text{DMSO}-d_6$) δ 143.68, 142.65, 130.21, 122.43, 118.16, 117.49, 64.49, 64.43, 48.53, 40.52 and 17.94.

4.5. 1-(3,4-Ethylenedioxy-5-bromophenyl)-2-aminopropane hydrochloride (16)

To a suspension of LiAlH_4 (0.85 g, 22.4 mmol) in dry diethyl ether (6 mL), cooled in a dry ice/acetone bath at -10 °C, was added dropwise a solution of 1-(3,4-ethylenedioxy-5-bromophenyl)-2-nitropropene (**5**) (1.23 g, 4.3 mmol) in dry diethyl ether (12 mL) and benzene (8 mL). The suspension was stirred for 5 h at 0 °C in

ice water, the excess hydride was decomposed by careful addition of water, the mixture was extracted with diethyl ether (3 \times 25 mL), the organic extracts were dried over MgSO_4 and rotary evaporated. The residue was then dissolved in dry diethyl ether and the hydrochloride (**16**) precipitated by passing gaseous HCl through the solution. Yield 30%, mp 148–150 °C. Anal. Calcd for $\text{C}_{11}\text{H}_{14}\text{BrNO}_2\cdot\text{HCl}\cdot 1/2\text{H}_2\text{O}$: C, 41.59; H, 5.08; N, 4.41. Found: C, 41.84; H, 4.88; N, 4.26. IR (KBr): ν_{\max} 3450, 2950, 1600, 1480, 1300, 1200 and 1080 cm^{-1} . ^1H NMR ($\text{DMSO}-d_6$) δ 8.02 (3H, s, NH_3^+); 6.94 (1H, d, $J = 2.3$ Hz, H-6); 6.72 (1H, d, $J = 2.3$ Hz, H-2); 4.20 (4H, s, CH_2O); 3.42 (1H, m, $\text{CH}_2\text{CH}(\text{CH}_3)\text{NH}_3^+$); 3.00 (1H, m, $\text{CH}_2\text{CH}(\text{CH}_3)\text{NH}_3^+$); 2.78 (1H, m, $\text{CH}_2\text{CH}(\text{CH}_3)\text{NH}_3^+$); 1.03 (3H, d, $J = 6.3$ Hz, $\text{CH}_2\text{CH}(\text{CH}_3)\text{NH}_3^+$). ^{13}C NMR ($\text{DMSO}-d_6$) δ 145.82, 141.06, 132.15, 126.67, 119.11, 114.10, 66.37, 65.57, 49.43, 36.52 and 15.16.

Following the same procedure described above for compound **16**, the aminopropane hydrochlorides **17–25** were obtained from the corresponding nitropropenes **6–14**. In this way the following compounds were prepared.

4.5.1. 1-(2-Thienyl)-2-aminopropane hydrochloride (17). Yield 63%, mp 143–145 °C (lit.¹³ 146 °C). ^1H NMR ($\text{DMSO}-d_6$ and D_2O) δ 7.23 (1H, m, H-5); 6.90 (2H, m, H-3 and H-4); 3.55 (1H, m, $\text{CH}_2\text{CH}(\text{CH}_3)\text{NH}_3^+$); 3.08 (2H, m, $\text{CH}_2\text{CH}(\text{CH}_3)\text{NH}_3^+$); 1.21 (3H, d, $J = 6.5$ Hz, $\text{CH}_2\text{CH}(\text{CH}_3)\text{NH}_3^+$).

4.5.2. 1-(3-Thienyl)-2-aminopropane hydrochloride (18). Yield 57%, mp 135–137 °C HRMS m/z 141.0619, calcd for $\text{C}_7\text{H}_{11}\text{NS}$, 141.0612. IR (KBr): ν_{\max} 2950, 1600, 1500, 1380, 1000, 720 and 680 cm^{-1} . ^1H NMR (D_2O) δ 7.35 (1H, dd, $J = 4.9$ Hz, $J' = 2.9$ Hz, H-5); 7.15 (1H, dd, $J = 2.9$ Hz, $J' = 1.1$ Hz, H-2); 6.94 (1H, dd, $J = 4.9$ Hz, $J' = 1.1$ Hz, H-4); 3.41 (1H, m, $\text{CH}_2\text{CH}(\text{CH}_3)\text{NH}_3^+$); 2.80 (2H, m, $\text{CH}_2\text{CH}(\text{CH}_3)\text{NH}_3^+$); 1.11 (3H, d, $J = 6.6$ Hz, $\text{CH}_2\text{CH}(\text{CH}_3)\text{NH}_3^+$).

4.5.3. 1-(2-Furyl)-2-aminopropane hydrochloride (19). Yield 32%, mp 120–121 °C. HRMS m/z 125.0838, calcd for $\text{C}_7\text{H}_{11}\text{NO}$, 125.0841. IR (KBr): ν_{\max} 3422, 3000, 1593, 1493, 1392, 1014 and 765 cm^{-1} . ^1H NMR ($\text{DMSO}-d_6$) δ 8.25 (3H, s, NH_3^+); 7.36 (1H, dd, $J = 2.1$ Hz, $J' = 0.7$ Hz, H-3); 6.30 (1H, dd, $J = 3.3$ Hz, $J' = 2.1$ Hz, H-4); 6.18 (1H, dd, $J = 3.3$ Hz, $J' = 0.7$ Hz, H-5); 3.55 (1H, m, $\text{CH}_2\text{CH}(\text{CH}_3)\text{NH}_3^+$); 2.87 (2H, m, $\text{CH}_2\text{CH}(\text{CH}_3)\text{NH}_3^+$); 1.19 (3H, d, $J = 6.5$ Hz, $\text{CH}_2\text{CH}(\text{CH}_3)\text{NH}_3^+$). ^{13}C NMR ($\text{DMSO}-d_6$) δ 152.10, 143.92, 112.33, 109.28, 47.40, 33.88 and 19.03.

4.5.4. 1-(3-Furyl)-2-aminopropane hydrochloride (20). Yield 38%, mp 125–127 °C. HRMS m/z 125.0830, calcd for $\text{C}_7\text{H}_{11}\text{NO}$, 125.0841. IR (KBr): ν_{\max} 3400, 2950, 1600, 1500, 1400, 1020 and 800 cm^{-1} . ^1H NMR ($\text{DMSO}-d_6$) δ 8.28 (3H, s, NH_3^+); 7.60 (1H, br s, H-5); 7.54 (1H, br s, H-2); 6.24 (1H, br s, H-4); 3.30 (1H, m, $\text{CH}_2\text{CH}(\text{CH}_3)\text{NH}_3^+$); 2.80 (2H, dd, $J = 4.8$ Hz, $J' = 14.1$ Hz, $\text{CH}_2\text{CH}(\text{CH}_3)\text{NH}_3^+$); 2.57 (2H, dd, $J = 9.1$ Hz, $J' = 14.1$ Hz, $\text{CH}_2\text{CH}(\text{CH}_3)\text{NH}_3^+$); 1.13 (3H, d, $J = 6.4$ Hz, $\text{CH}_2\text{CH}(\text{CH}_3)\text{NH}_3^+$). ^{13}C NMR

(DMSO- d_6) δ 143.44, 140.56, 119.67, 111.31, 46.92, 29.39 and 17.61.

4.5.5. 1-(4-Bromo-2-thienyl)-2-aminopropane hydrochloride (21). Yield 31%, mp 165–167 °C. Anal. Calcd for $C_7H_{10}BrNS \cdot HCl$: C, 32.77; H, 4.32; N, 5.46; S, 12.49. Found: C, 33.32; H, 3.94; N, 5.58; S, 11.76. IR (KBr): ν_{max} 3400, 2900, 1600, 1520, 1380, 1100 and 800 cm^{-1} . 1H NMR (DMSO- d_6) δ 8.26 (3H, s, NH_3^+); 7.54 (1H, s, H-5); 7.01 (1H, s, H-3); 3.37 (1H, m, $CH_2CH(CH_3)NH_3^+$); 3.19 (1H, dd, $J = 14.5$ Hz, $J' = 5.5$ Hz, $CH_2CH(CH_3)NH_3^+$); 2.97 (1H, dd, $J = 14.5$ Hz, $J' = 8.4$ Hz, $CH_2CH(CH_3)NH_3^+$); 1.17 (3H, d, $J = 6.5$ Hz, $CH_2CH(CH_3)NH_3^+$). ^{13}C NMR (DMSO- d_6) δ 141.13, 129.77, 123.47, 109.11, 48.40, 34.62 and 18.27.

4.5.6. 1-(5-Bromo-2-thienyl)-2-aminopropane hydrochloride (22). Yield 43%, mp 122–124 °C. Anal. Calcd for $C_7H_{10}BrNS \cdot HCl$: C, 32.77; H, 4.32; N, 5.46; S, 12.49. Found: C, 33.13; H, 4.40; N, 5.60; S, 12.09. IR (KBr): ν_{max} 3400, 2950, 1600, 1450, 1400 and 800 cm^{-1} . 1H NMR (DMSO- d_6) δ 8.19 (3H, s, NH_3^+); 7.01 (1H, d, $J = 3.4$ Hz, H-3); 6.76 (1H, d, $J = 3.4$ Hz, H-4); 3.42 (1H, m, $CH_2CH(CH_3)NH_3^+$); 3.08 (1H, dd, $J = 14.9$ Hz, $J' = 5.2$ Hz, $CH_2CH(CH_3)NH_3^+$); 2.85 (1H, dd, $J = 14.9$ Hz, $J' = 8.6$ Hz, $CH_2CH(CH_3)NH_3^+$); 1.09 (3H, d, $J = 6.9$ Hz, $CH_2CH(CH_3)NH_3^+$).

4.5.7. 1-(5-Bromo-2-furyl)-2-aminopropane hydrochloride (23). Yield 37%, mp 124–126 °C. HRMS m/z 202.9953, calcd for $C_7H_{11}BrNO$, 202.9925. IR (KBr): ν_{max} 3400, 2950, 1600, 1500, 1400, 1200 and 800 cm^{-1} . 1H NMR (DMSO- d_6) δ 8.26 (3H, s, NH_3^+); 6.49 (1H, d, $J = 3.3$ Hz, H-4); 6.35 (1H, d, $J = 3.3$ Hz, H-3); 3.40 (1H, m, $CH_2CH(CH_3)NH_3^+$); 3.04 (1H, dd, $J = 15.0$ Hz, $J' = 5.3$ Hz, $CH_2CH(CH_3)NH_3^+$); 2.83 (1H, dd, $J = 15.0$ Hz, $J' = 8.4$ Hz, $CH_2CH(CH_3)NH_3^+$); 1.18 (3H, d, $J = 6.6$ Hz, $CH_2CH(CH_3)NH_3^+$). ^{13}C NMR (DMSO- d_6) δ 153.35, 120.64, 113.11, 111.70, 46.57, 33.16 and 18.44.

4.5.8. 1-(3-Benzothieryl)-2-aminopropane hydrochloride (24). Yield 52%, mp 189–191 °C. HRMS m/z 191.0796, calcd for $C_{11}H_{13}NS$, 191.0769. IR (KBr): ν_{max} 3412, 3025, 1598, 1570, 1458, 1022, 758 and 738 cm^{-1} . 1H NMR (DMSO- d_6) δ 7.83 (1H, m, H-5); 7.75 (1H, m, H-6); 7.33 (3H, m, H-2, H-4 and H-7); 3.54 (1H, m, $CH_2CH(CH_3)NH_3^+$); 3.11 (1H, m, $CH_2CH(CH_3)NH_3^+$); 2.99 (1H, m, $CH_2CH(CH_3)NH_3^+$); 1.13 (3H, d, $J = 6.5$ Hz, $CH_2CH(CH_3)NH_3^+$).

4.5.9. 1-(2-Benzofuryl)-2-aminopropane hydrochloride (25). Yield 26%, mp 151–153 °C. Anal. Calcd for $C_{11}H_{13}NO \cdot HCl$: C, 62.41; H, 6.67; N, 6.62. Found: C, 62.48; H, 6.71; N, 6.37. IR (KBr): ν_{max} 3400, 2900, 1600, 1450, 1050, 800 and 750 cm^{-1} . 1H NMR (DMSO- d_6) δ 8.33 (3H, s, NH_3^+); 7.53 (2H, m, H-4 and H-7); 7.22 (2H, m, H-5 and H-6); 6.76 (1H, s, H-3); 3.55 (1H, m, $CH_2CH(CH_3)NH_3^+$); 3.22 (1H, dd, $J = 14.9$ Hz, $J' = 5.4$ Hz, $CH_2CH(CH_3)NH_3^+$); 3.01 (1H, dd, $J = 14.9$ Hz, $J' = 8.5$ Hz, $CH_2CH(CH_3)NH_3^+$); 1.24 (3H, d, $J = 6.4$ Hz, $CH_2CH(CH_3)NH_3^+$). ^{13}C NMR

(DMSO- d_6) δ 154.28, 153.91, 128.27, 123.77, 122.74, 120.68, 110.83, 104.82, 45.60, 32.87 and 17.99.

4.6. Evaluation of the inhibitory activity of the heteroarylaminopropanes

The inhibitory activity of all compounds vis-à-vis MAO-A and MAO-B was assayed in vitro following a protocol described previously.¹⁴ Briefly, mitochondrial suspensions from rat brain (male Sprague Dawley rats weighing 180–230 g, sacrificed by decapitation) were employed as a source of crude MAO. The activities of both isoforms in the presence of variable concentrations of the inhibitors were measured in triplicate by HPLC with electrochemical detection (Merck-Hitachi L-7110 pump with a Lichrospher C18 5 μm column and a Labchrom L-3500A amperometric detector). Serotonin (5-HT, 100 μM) or 4-dimethylaminophenethylamine (4-DMAPEA, 5 μM)²³ were used as selective substrates for MAO-A and MAO-B, respectively. Control experiments were carried out without inhibitor and blanks were run without mitochondrial suspension. The heights of the chromatographic peaks of 5-HT, DMAPEA and their main MAO metabolites (5-hydroxyindolacetic acid and 4-dimethylaminophenylacetic acid) were used to calculate MAO activity. IC_{50} values were determined using the Prism Graph Pad software, from plots of inhibition percentages (calculated in relation to a sample of the enzyme treated under the same conditions without inhibitors) versus the logarithm of the inhibitor concentration.

The time course of MAO inhibition by the drugs was assessed by preincubating the reaction mixture with different inhibitors at 37 °C for 30 min. In all cases the employed inhibitor concentrations, without preincubation, produced only partial enzyme inhibition. Percent inhibition of deamination of 5-HT (100 μM) was determined by HPLC with electrochemical detection. After preincubation, MAO activity was measured as described.¹⁴

4.7. Molecular simulation

The crystallographic data of MAO-A (PDB: 1O5W) were used for all calculations. The hydrogen atoms of the protein and the FAD molecule were built using Insight II²⁴ and then were relaxed following a minimization protocol using Discover_3²⁴ and the force field ESFF. The calculations were performed using a distance-dependent dielectric constant of 80. All docking simulations were performed with Autodock 3.02.²⁵ The protein and substrate were assigned partial charges using the force field ESFF. Atomic solvation parameters and fragmental volumes were assigned to the protein atoms using the addsol option. The grid maps were calculated using autogrid3 and were centred on the putative ligand-binding site. The volume chosen for the grid maps were made up of 40 \times 40 \times 40 points, with a grid-point spacing of 0.375 Å. The autotors option was used to define the rotating bonds in the ligand. In the Lamarckian genetic algorithm (LGA) dockings, an initial population of random individuals with a population

size of 50 individuals, a maximum number of 1.5×10^6 energy evaluations, a maximum number of generations of 27,000, a mutation rate of 0.02, and a cross-over rate of 0.80 were employed. Proportional selection was used, where the average worst energy was calculated over a window of the previous 10 generations. In the LGA dockings, the pseudo-Solis and Wets local search method was used, with a maximum of 300 iterations per local search. The probability of performing local search on an individual in the population was 0.06. The docked compound complexes were built using the lowest free-energy binding positions.

Acknowledgments

This work was supported by DICYT-USACH and by Fondecyt project 1000776.

References and notes

1. Binda, C.; Newton-Vinson, P.; Hubálek, F.; Edmondson, D. E.; Mattevi, A. *Nat. Struct. Biol.* **2002**, *9*, 22.
2. Binda, C.; Li, M.; Hubálek, F.; Restelli, N.; Edmondson, D. E.; Mattevi, A. *Proc. Natl. Acad. Sci. U.S.A.* **2003**, *100*, 9750.
3. Binda, C.; Hubálek, F.; Li, M.; Edmondson, D. E.; Mattevi, A. *FEBS Lett.* **2004**, *564*, 225.
4. Ma, J.; Yoshimura, M.; Yamashita, E.; Nakagawa, A.; Ito, A.; Tsukihara, T. *J. Mol. Biol.* **2004**, *338*, 103.
5. Reyes-Parada, M.; Fierro, A.; Iturriaga-Vásquez, P.; Cassels, B. K. *Curr. Enzyme Inhib.* **2005**, *1*, 85.
6. Vallejos, G.; Rezende, M. C.; Cassels, B. K. *J. Comput. Aided Mol. Des.* **2002**, *16*, 95.
7. Osorio-Olivares, M.; Rezende, M. C.; Sepúlveda-Boza, S.; Cassels, B. K.; Fierro, A. *Bioorg. Med. Chem.* **2004**, *12*, 4055.
8. Yoshida, S.; Meyer, O. G.; Rosen, T. C.; Haufe, G.; Ye, S.; Sloan, M. J.; Kirk, K. L. *J. Med. Chem.* **2004**, *47*, 1796.
9. Yoshida, S.; Rosen, T. C.; Meyer, O. G.; Sloan, M. J.; Ye, S.; Haufe, G.; Kirk, K. L. *Bioorg. Med. Chem.* **2004**, *12*, 2645.
10. Morón, J. A.; Pérez, V.; Pastó, M.; Lizcano, J. M.; Unzeta, M. *J. Pharmacol. Exp. Ther.* **2000**, *292*, 788.
11. Kagaya, T.; Kajiwara, A.; Nagato, S.; Akasaka, K.; Kubota, A. *J. Pharmacol. Exp. Ther.* **1996**, *278*, 243.
12. Wouters, J. *Curr. Med. Chem.* **1998**, *5*, 137.
13. Conde, S.; Madroño, R.; Fernández-Tomé, M. P.; del Rio, J. *J. Med. Chem.* **1978**, *21*, 978.
14. Scorza, M. C.; Carrau, C.; Silveira, R.; Zapata-Torres, G.; Cassels, B. K.; Reyes-Parada, M. *Biochem. Pharmacol.* **1997**, *54*, 1361.
15. Gallardo-Godoy, A.; Fierro, A.; McLean, T. H.; Castillo, M.; Cassels, B. K.; Reyes-Parada, M.; Nichols, D. E. *J. Med. Chem.* **2005**, *48*, 2407.
16. Bernstein, F. C.; Koetzle, T. F.; Williams, G. J.; Meyer, E. F., Jr.; Brice, M. D.; Rodgers, J. R.; Kennard, O.; Shimanouchi, T.; Tasumi, M. *J. Mol. Biol.* **1977**, *112*, 535.
17. Nagatsu, T. *Neurotoxicology* **2004**, *25*, 11.
18. Geha, R. M.; Rebrin, I.; Chen, K.; Shih, J. C. *J. Biol. Chem.* **2001**, *276*, 9877.
19. Tsugeno, Y.; Ito, A. *J. Biol. Chem.* **1997**, *272*, 14033.
20. Geha, R. M.; Chen, K.; Shih, J. C. *J. Neurochem.* **2000**, *75*, 1304.
21. Thi, B. T. L.; Iiyama, K.; Stone, B. A. *Phytochemistry* **1996**, *41*, 1507.
22. Kurata, K.; Amiya, T. *Bull. Chem. Soc. Jpn.* **1980**, *53*, 2020.
23. Reyes-Parada, M.; Scorza, M. C.; Silveira, R.; Dajas, F.; Cassels, B. K. *Life Sci.* **1994**, *54*, 1955.
24. Insight II and Discover, User Guide, Accelrys, San Diego, CA, 1998.
25. Morris, G. M.; Goodsell, D. S.; Halliday, R. S.; Huey, R.; Hart, W. E.; Belew, R. K.; Olson, A. J. *J. Comput. Chem.* **1998**, *19*, 1639.